Neutron star matter with Δ isobars in a relativistic quark model

Himanshu S. Sahoo,[1] Gautam Mitra,[1] Rabindranath Mishra,[1] Prafulla K. Panda,[2] and Bao-An Li[3]
[1]*Department of Physics, Ravenshaw University, Cuttack 753 003, India*
[2]*Department of Physics, Utkal University, Bhubaneswar 751 004, India*
[3]*Department of Physics and Astronomy, Texas A&M University–Commerce, Commerce, Texas 75429-3011, USA*

(Received 8 February 2018; revised manuscript received 28 August 2018; published 3 October 2018)

The possibility of the appearance of Δ(1232) isobars in neutron star matter and the so-called Δ *puzzle* is investigated in a relativistic quark model where the confining interaction for quarks inside a baryon is represented by a phenomenological average potential in an equally mixed scalar-vector harmonic form. The hadron-hadron interaction in nuclear matter is then realized by introducing additional quark couplings to σ, ω, and ρ mesons through mean-field approximations. The hyperon couplings are fixed from the hyperon optical potentials at saturation density. Effects of moderate variations in the Δ-ω and Δ-ρ coupling strengths on the critical density of forming Δ resonances and on the mass-radius relation of neutron stars is studied. We have also made an attempt to study the impact of in-medium mass variations of the Δ baryon on the structure of neutron stars. It is observed that, within the constraints of the masses of the precisely measured massive pulsars PSR J0348+0432 and PSR J1614−2230, neutron stars with a composition of both Δ isobars and hyperons are possible in the present model.

DOI: 10.1103/PhysRevC.98.045801

I. INTRODUCTION

The formation of baryons heavier than nucleons at the core of a neutron star, and the effects of such formation on the mass and radius of the neutron star, are subjects of active research in nuclear astrophysics. It is expected that high density neutron star matter may consist not only of nucleons and leptons but also several exotic components such as hyperons and mesons as well as quark matter in different forms and phases. While many studies have been conducted to address the appearance of hyperons and on the so-called *hyperon puzzle* [1–18], little work has been done to study the appearance of Δ(1232) isobars in neutron stars. An earlier work [1] indicated the appearance of Δ at much higher densities than the typical densities of the core of a neutron star and hence was considered of little significance to astrophysical studies. However, recent studies [19–26] suggest the possibility of an early appearance of Δ isobars. In fact, the critical density $\rho_{\Delta^-}^{\rm crit}$ of appearance of Δ^- in these studies is around 2 to 3 times the nuclear saturation density ρ_0. Such an early appearance leads to the softening of the equation of state (EOS) of dense matter, consequently reducing the maximum mass of neutron stars below the current observational limit of $(2.01 \pm 0.04)M_\odot$ (PSR J0348+0432) [27] and $(1.928 \pm 0.017)M_\odot$ (PSR J1614−2230) [28,29].

In the present work, we would like to address the Δ-puzzle in a relativistic quark model, alternatively called the modified quark-meson coupling model (MQMC). The MQMC model is based on a confining relativistic independent quark potential model rather than a bag to describe the baryon structure in vacuum. The baryon-baryon interactions are realized by making additional quark couplings to σ, ω, and ρ mesons through mean-field approximations. This relativistic quark model has been successfully applied to various domains of nuclear and high energy physics, including baryon spectroscopy [30], electromagnetic form factors of nucleons [31], magnetic moments of the octet baryons [32], nucleon structure functions in deep inelastic scattering [33], and symmetric [34] and asymmetric [35] nuclear matter. More recently this framework has been used to study the equation of state of neutron star matter with hyperon degrees of freedom and the properties of Λ and Ξ^0 hypernuclei [36,37]. Studies on the effect of the nucleon charge radius on the mass and radius of neutron stars [38] and developing an equation of state within the constraints set by GW170817 observations [39] are some other recent works undertaken using this model.

In the present work we include the delta isobars (Δ^-, Δ^0, Δ^+, Δ^{++}) together with hyperons as new degrees of freedom in dense hadronic matter relevant for neutron stars. The interactions between nucleons, Δ's, and hyperons in dense matter is studied and the possibility of the existence of the Δ baryon at densities relevant to a neutron star core as well as its effects on the mass of the neutron star is analyzed. In free-space, the two-body nucleon-nucleon (NN) interaction is reasonably well known below the pion production threshold. In-medium NN interaction even at saturation density, especially the isovector part, and spin-isospin and spin-orbit coupling are not well known. The saturation properties of nuclear matter at ρ_0 and properties of finite nuclei have not fixed all these properties of NN interaction yet. The extrapolation of such interactions to densities beyond nuclear saturation density is quite challenging. The hyperon-nucleon interaction are known experimentally, but large uncertainties exist. Studies indicate a repulsive Σ nuclear potential and a shallow attractive potential for Ξ. We use the hyperon optical potential values of $U_\Lambda = -28$ MeV [40,41], $U_\Sigma = 30$ MeV [9,11,42–44], and $U_\Xi = -10$ MeV at saturation respectively for the Λ, Σ, and

Ξ hyperons. We also study the effect of variation of the U_Ξ from -10 to -18 MeV [9–11,42,43] on the star properties.

Due to lack of microscopic constraints on the coupling of the Δ baryon with ω and ρ mesons, many workers take the coupling strength of the mesons with Δ to be the same as that of the nucleons. Studies [45] based on the quark counting argument suggest universal couplings between nucleons, Δ isobars, and mesons, giving the values of $x_{\omega\Delta} = g_{\omega\Delta}/g_{\omega N} = 1$ and $x_{\sigma\Delta} = g_{\sigma\Delta}/g_{\sigma N} = 1$. Theoretical studies of Gamow-Teller transitions and $M1$ giant resonance in nuclei by Bohr and Mottelson [46] observed a 25–40% reduction in transition strength due to the couplings to Δ isobars, indicating weaker coupling of the isoscalar mesons to the Δ isobars. Further, the difference between $x_{\sigma\Delta}$ and $x_{\omega\Delta}$ was found to be $x_{\sigma\Delta} - x_{\omega\Delta} = 0.2$ in the Hartree approximation [47]. In the present work we fix the Δ-ω coupling with the value of $x_{\omega\Delta} = 0.7$. We also study the effect of moderate variations in the value of $x_{\omega\Delta}$ and $x_{\rho\Delta}$ on the critical density of appearance of Δ^- baryons as well as on the mass and radius of neutron stars.

The paper is organized as follows: In Sec. II, a brief outline of the model describing the baryon structure in vacuum is discussed. The baryon mass is then realized by appropriately taking into account the center-of-mass correction, pionic correction, and gluonic correction. The EOS with the inclusion of the Δ isobars and the hyperons is then developed in Sec. III. The results and discussions are made in Sec. IV. We summarize our findings in Sec. V.

II. MODIFIED QUARK MESON COUPLING MODEL

The modified quark-meson coupling model has been successful in obtaining various bulk properties of symmetric and asymmetric nuclear matter as well as hyperonic matter within the accepted constraints [34–36]. We now extend this model to include the Δ isobars (Δ^-, Δ^0, Δ^+, Δ^{++}) along with nucleons and hyperons in neutron star matter under conditions of β equilibrium and charge neutrality. We begin by considering baryons as composed of three constituent quarks confined inside the hadron core by a phenomenological flavor-independent potential, $U(r)$. Such a potential may be expressed as an admixture of equal scalar and vector parts in harmonic form [34],

$$U(r) = \tfrac{1}{2}(1+\gamma^0)V(r),$$

with

$$V(r) = (ar^2 + V_0), \quad a > 0. \tag{1}$$

Here (a, V_0) are the potential parameters. The confining interaction provides the zeroth-order quark dynamics of the hadron. In the medium, the quark field $\psi_q(\mathbf{r})$ satisfies the Dirac equation

$$\left[\gamma^0\left(\epsilon_q - V_\omega - \tfrac{1}{2}\tau_{3q}V_\rho\right) - \vec{\gamma}\cdot\vec{p} - (m_q - V_\sigma) - U(r)\right]\psi_q(\vec{r}) = 0, \tag{2}$$

where $V_\sigma = g^q_\sigma\sigma_0$, $V_\omega = g^q_\omega\omega_0$, and $V_\rho = g^q_\rho b_{03}$. Here σ_0, ω_0, and b_{03} are the classical meson fields, and g^q_σ, g^q_ω, and g^q_ρ are the quark couplings to the σ, ω, and ρ mesons, respectively. m_q is the quark mass and τ_{3q} is the third component of the isospin matrix. We can now define

$$\epsilon'_q = (\epsilon^*_q - V_0/2) \quad \text{and} \quad m'_q = (m^*_q + V_0/2), \tag{3}$$

where the effective quark energy $\epsilon^*_q = \epsilon_q - V_\omega - \frac{1}{2}\tau_{3q}V_\rho$ and effective quark mass $m^*_q = m_q - V_\sigma$. We now introduce λ_q and r_{0q} as

$$(\epsilon'_q + m'_q) = \lambda_q \quad \text{and} \quad r_{0q} = (a\lambda_q)^{-\frac{1}{4}}. \tag{4}$$

The ground-state quark energy can be obtained from the eigenvalue condition

$$(\epsilon'_q - m'_q)\sqrt{\frac{\lambda_q}{a}} = 3. \tag{5}$$

The solution of (5) for the quark energy ϵ^*_q immediately leads to the mass of baryon in the medium in zeroth order as

$$E^{*0}_B = \sum_q \epsilon^*_q. \tag{6}$$

We next consider the spurious center-of-mass correction $\epsilon_{\text{c.m.}}$, the pionic correction δM^π_B for restoration of chiral symmetry, and the short-distance one-gluon exchange contribution $(\Delta E_B)_g$ to the zeroth-order baryon mass in the medium.

We have used a fixed center potential to calculate the wave functions of a quark in a baryon. To study the properties of the baryon constructed from these quarks, we must extract the contribution of the center-of-mass motion in order to obtain physically relevant results. Here, we extract the center-of-mass energy to first order in the difference between the fixed center and relative quark coordinate, using the method described by Guichon *et al.* [48,49]. The center-of-mass correction is given by

$$e_{\text{c.m.}} = e^{(1)}_{\text{c.m.}} + e^{(2)}_{\text{c.m.}}, \tag{7}$$

where

$$e^{(1)}_{\text{c.m.}} = \sum_{i=1}^{3}\left[\frac{m_{q_i}}{\sum_{k=1}^{3} m_{q_k}}\frac{6}{r^2_{0q_i}(3\epsilon'_{q_i} + m'_{q_i})}\right], \tag{8}$$

$$e^{(2)}_{\text{c.m.}} = \frac{a}{2}\Bigg[\frac{2}{\sum_k m_{q_k}}\sum_i m_i\langle r_i^2\rangle + \frac{2}{\sum_k m_{q_k}}\sum_i m_i\langle\gamma^0(i)r_i^2\rangle - \frac{3}{\left(\sum_k m_{q_k}\right)^2}\sum_i m_i^2\langle r_i^2\rangle - \frac{1}{\left(\sum_k m_{q_k}\right)^2} \times \sum_i\langle\gamma^0(1)m_i^2r_i^2\rangle - \frac{1}{\left(\sum_k m_{q_k}\right)^2}\sum_i\langle\gamma^0(2)m_i^2r_i^2\rangle - \frac{1}{\left(\sum_k m_{q_k}\right)^2}\sum_i\langle\gamma^0(3)m_i^2r_i^2\rangle\Bigg]. \tag{9}$$

In the above, we have used $i = (u, d, s)$ and $k = (u, d, s)$, and the various quantities are defined as

$$\langle r_i^2\rangle = \frac{(11\epsilon'_{qi} + m'_{qi})r^2_{0qi}}{2(3\epsilon'_{qi} + m'_{qi})}, \tag{10}$$

$$\langle\gamma^0(i)r_i^2\rangle = \frac{(\epsilon'_{qi} + 11m'_{qi})r^2_{0qi}}{2(3\epsilon'_{qi} + m'_{qi})}, \tag{11}$$

$$\langle \gamma^0(i) r_j^2 \rangle_{i\neq j} = \frac{(\epsilon'_{qi} + 3m'_{qi})\langle r_j^2\rangle}{3\epsilon'_{qi} + m'_{qi}}. \quad (12)$$

The pionic corrections in the model for the nucleons become

$$\delta M_N^\pi = -\frac{171}{25} I_\pi f_{NN\pi}^2, \quad (13)$$

where $f_{NN\pi}$ is the pseudovector nucleon-pion coupling constant. Taking $w_k = (k^2 + m_\pi^2)^{1/2}$, the I_π becomes

$$I_\pi = \frac{1}{\pi {m_\pi}^2} \int_0^\infty dk \frac{k^4 u^2(k)}{w_k^2}, \quad (14)$$

with the axial vector nucleon form factor given as

$$u(k) = \left[1 - \frac{3}{2}\frac{k^2}{\lambda_q(5\epsilon'_q + 7m'_q)}\right] e^{-k^2 r_0^2/4}. \quad (15)$$

The pionic correction for Σ^0 and Λ^0 become

$$\delta M_{\Sigma^0}^\pi = -\frac{12}{5} f_{NN\pi}^2 I_\pi, \quad (16)$$

$$\delta M_{\Lambda^0}^\pi = -\frac{108}{25} f_{NN\pi}^2 I_\pi. \quad (17)$$

Similarly the pionic correction for Σ^- and Σ^+ is

$$\delta M_{\Sigma^+,\Sigma^-}^\pi = -\frac{12}{5} f_{NN\pi}^2 I_\pi. \quad (18)$$

The pionic correction for Ξ^0 and Ξ^- is

$$\delta M_{\Xi^-,\Xi^0}^\pi = -\frac{27}{25} f_{NN\pi}^2 I_\pi. \quad (19)$$

For Δ baryon, the pionic correction is given by

$$\delta M_\Delta^\pi = -\frac{99}{25} f_{NN\pi}^2 I_\pi. \quad (20)$$

The one-gluon exchange interaction is provided by the interaction Lagrangian density

$$\mathcal{L}_I^g = \sum J_i^{\mu a}(x) A_\mu^a(x), \quad (21)$$

where $A_\mu^a(x)$ are the octet gluon vector-fields and $J_i^{\mu a}(x)$ is the ith quark color current. The gluonic correction can be separated into two pieces, namely, one from the color electric field (E_i^a) and another from the magnetic field (B_i^a) generated by the ith quark color current density

$$J_i^{\mu a}(x) = g_c \bar{\psi}_q(x) \gamma^\mu \lambda_i^a \psi_q(x), \quad (22)$$

with λ_i^a being the usual Gell-Mann SU(3) matrices and $\alpha_c = g_c^2/4\pi$. The contribution to the mass can be written as a sum of color-electric and color-magnetic parts as

$$(\Delta E_B)_g = (\Delta E_B)_g^E + (\Delta E_B)_g^M. \quad (23)$$

Finally, taking into account the specific quark flavor and spin configurations in the ground state baryons and using the relations $\langle \sum_a (\lambda_i^a)^2 \rangle = 16/3$ and $\langle \sum_a (\lambda_i^a \lambda_j^a) \rangle_{i\neq j} = -8/3$ for baryons, one can write the energy correction due to color electric contribution as given in [36],

$$(\Delta E_B)_g^E = \alpha_c \left(b_{uu} I_{uu}^E + b_{us} I_{us}^E + b_{ss} I_{ss}^E\right), \quad (24)$$

TABLE I. The coefficients a_{ij} and b_{ij} used in the calculation of the color-electric and and color-magnetic energy contributions due to one-gluon exchange.

Baryon	a_{uu}	a_{us}	a_{ss}	b_{uu}	b_{us}	b_{ss}
N	−3	0	0	0	0	0
Δ	3	0	0	0	0	0
Λ	−3	0	0	1	−2	1
Σ	1	−4	0	1	−2	1
Ξ	0	−4	1	1	−2	1

and that due to color magnetic contributions as

$$(\Delta E_B)_g^M = \alpha_c \left(a_{uu} I_{uu}^M + a_{us} I_{us}^M + a_{ss} I_{ss}^M\right), \quad (25)$$

where a_{ij} and b_{ij} are the numerical coefficients depending on each baryon and are given in Table I. In the above, we have

$$I_{ij}^E = \frac{16}{3\sqrt{\pi}} \frac{1}{R_{ij}} \left[1 - \frac{\alpha_i + \alpha_j}{R_{ij}^2} + \frac{3\alpha_i \alpha_j}{R_{ij}^4}\right],$$
$$I_{ij}^M = \frac{256}{9\sqrt{\pi}} \frac{1}{R_{ij}^3} \frac{1}{(3\epsilon'_i + m'_i)} \frac{1}{(3\epsilon'_j + m'_j)}, \quad (26)$$

where

$$R_{ij}^2 = 3\left[\frac{1}{\left(\epsilon_i^{'2} - m_i^{'2}\right)} + \frac{1}{\left(\epsilon_j^{'2} - m_j^{'2}\right)}\right],$$
$$\alpha_i = \frac{1}{(\epsilon'_i + m'_i)(3\epsilon'_i + m'_i)}. \quad (27)$$

The color electric contributions to the bare mass for nucleon and the Δ baryon are $(\Delta E_N)_g^E = 0$ and $(\Delta E_\Delta)_g^E = 0$. Therefore the one-gluon contribution for Δ becomes

$$(\Delta E_\Delta)_g^M = \frac{256\alpha_c}{3\sqrt{\pi}} \left[\frac{1}{(3\epsilon'_u + m'_u)^2 R_{uu}^3}\right]. \quad (28)$$

The details of the gluonic correction for the nucleons and hyperons are given in [36].

Treating all energy corrections independently, the mass of the baryon in the medium becomes

$$M_B^* = E_B^{*0} - \epsilon_{\text{c.m.}} + \delta M_B^\pi + (\Delta E_B)_g^E + (\Delta E_B)_g^M. \quad (29)$$

III. THE EQUATION OF STATE

The total energy density and pressure at a particular baryon density, including all the members of the baryon octet and the Δ isobars, for the nuclear matter in β equilibrium can be found as

$$\mathcal{E} = \frac{1}{2} m_\sigma^2 \sigma_0^2 + \frac{1}{2} m_\omega^2 \omega_0^2 + \frac{1}{2} m_\rho^2 b_{03}^2$$
$$+ \frac{\gamma}{2\pi^2} \sum_B \int^{k_{f,B}} \left[k^2 + M_B^{*2}\right]^{1/2} k^2 dk$$
$$+ \sum_l \frac{1}{\pi^2} \int_0^{k_l} \left[k^2 + m_l^2\right]^{1/2} k^2 dk, \quad (30)$$

$$P = -\frac{1}{2}m_\sigma^2\sigma_0^2 + \frac{1}{2}m_\omega^2\omega_0^2 + \frac{1}{2}m_\rho^2 b_{03}^2 + \frac{\gamma}{6\pi^2}\sum_B \int^{k_{f,B}} \frac{k^4 dk}{\left[k^2 + M_B^{*2}\right]^{1/2}} + \frac{1}{3}\sum_l \frac{1}{\pi^2}\int_0^{k_l} \frac{k^4 dk}{\left[k^2 + m_l^2\right]^{1/2}}, \quad (31)$$

where γ is the spin degeneracy factor for nuclear matter. For the nucleons and hyperons $\gamma = 2$ and for the Δ baryons $\gamma = 4$. Here $B = N, \Delta, \Lambda, \Sigma^{\pm}, \Sigma^0, \Xi^-, \Xi^0$, and $l = e, \mu$.

The chemical potentials, necessary to define the β-equilibrium conditions, are given by

$$\mu_B = \sqrt{k_B^2 + M_B^{*2}} + g_\omega\omega_0 + g_\rho\tau_{3B}b_{03}, \quad (32)$$

where τ_{3B} is the isospin projection of the baryon B.

The lepton Fermi momenta are the positive real solutions of $(k_e^2 + m_e^2)^{1/2} = \mu_e$ and $(k_\mu^2 + m_\mu^2)^{1/2} = \mu_\mu$. The equilibrium composition of the star is obtained by solving the equations of motion of meson fields in conjunction with the charge neutrality condition, given in (33), at a given total baryonic density $\rho = \sum_B \gamma k_B^3/(6\pi^2)$. The effective masses of the baryons are obtained self-consistently in this model.

Since the neutron star timescale is quite long, we need to consider the occurrence of weak processes in its matter. Moreover, for stars in which the strongly interacting particles are baryons, the composition is determined by the requirements of charge neutrality and β-equilibrium conditions under the weak processes $B_1 \to B_2 + l + \overline{\nu}_l$ and $B_2 + l \to B_1 + \nu_l$. After deleptonization, the charge neutrality condition yields

$$q_{\rm tot} = \sum_B q_B \frac{\gamma k_B^3}{6\pi^2} + \sum_{l=e,\mu} q_l \frac{k_l^3}{3\pi^2} = 0, \quad (33)$$

where q_B corresponds to the electric charge of baryon species B and q_l corresponds to the electric charge of lepton species l. Since the timescale of a star is effectively infinite compared to the weak interaction timescale, weak interaction violates strangeness conservation. The strangeness quantum number is therefore not conserved in a star and the net strangeness is determined by the condition of β equilibrium, which for baryon B is then given by $\mu_B = b_B\mu_n - q_B\mu_e$, where μ_B is the chemical potential of baryon B and b_B is its baryon number. Thus the chemical potential of any baryon can be obtained from the two independent chemical potentials μ_n and μ_e of neutron and electron respectively.

In the present work, the baryon couplings are given by $g_{\omega B} = x_{\omega B}g_{\omega N}$ and $g_{\rho B} = x_{\rho B}g_{\rho N}$, where $x_{\omega B}$ and $x_{\rho B}$ are equal to 1 for the nucleons and acquire different values in different parametrizations for the other baryons. We mention here that the s quark is unaffected by the σ and ω mesons, i.e., $g_\sigma^s = g_\omega^s = 0$. We also note here that, in the present work, baryons are not considered as point particles. They have an internal structure, the state of which is realized in SU(6). In the present case we have considered SU(2) symmetry, taking the interaction of u quarks and d quarks with the mesons as identical. Here we fix g_σ^q (coupling constant for the quarks with the σ meson) to the saturation properties of nuclear matter self-consistently. It therefore does not give a direct definition of $g_{\sigma B}$ and hence of $x_{\sigma B}$ for baryons.

TABLE II. The potential parameter V_0 for different baryons obtained for the quark masses $m_u = m_d = 150$ MeV, $m_s = 230$ MeV with $a = 0.722970\,\text{fm}^{-3}$ and at quark masses $m_u = m_d = 200$ MeV, $m_s = 280$ MeV with $a = 0.795590\,\text{fm}^{-3}$.

Baryon	M_B (MeV)	V_0 (MeV) $m_{u,d} = 150$ MeV	V_0 (MeV) $m_{u,d} = 200$ MeV
N	939	36.76	5.44
Λ	1115.6	69.34	35.18
Σ	1193.1	86.10	50.78
Ξ	1321.3	104.64	67.13
Δ	1232	91.26	61.59

The vector mean fields ω_0 and b_{03} are determined through

$$\omega_0 = \frac{g_\omega}{m_\omega{}^2}\sum_B x_{\omega B}\rho_B, \quad b_{03} = \frac{g_\rho}{2m_\rho{}^2}\sum_B x_{\rho B}\tau_{3B}\rho_B, \quad (34)$$

where $g_\omega = 3g_\omega^q$ and $g_\rho = g_\rho^q$. Finally, the scalar mean field σ_0 is fixed by

$$\frac{\partial\mathcal{E}}{\partial\sigma_0} = 0. \quad (35)$$

The isoscalar-scalar and isoscalar-vector couplings g_σ^q and g_ω are fitted to the saturation density and binding energy for nuclear matter. The isovector-vector coupling g_ρ is set by fixing the symmetry energy at $J = 32.0$ MeV. For a given baryon density, ω_0, b_{03}, and σ_0 are calculated from (34) and (35), respectively.

The relation between the mass and radius of a star with its central energy density can be obtained by integrating the Tolman-Oppenheimer-Volkoff (TOV) equations [50,51] given by,

$$\frac{dP}{dr} = -\frac{G}{r}\frac{[\mathcal{E} + P][M + 4\pi r^3 P]}{(r - 2GM)}, \quad (36)$$

$$\frac{dM}{dr} = 4\pi r^2\mathcal{E}, \quad (37)$$

with G as the gravitational constant and $M(r)$ as the enclosed gravitational mass. We have used $c = 1$. Given an EOS, these equations can be integrated from the origin as an initial value problem for a given choice of the central energy density

TABLE III. Parameters for nuclear matter. They are determined from the binding energy per nucleon, $E_{B.E} = B_0 \equiv \mathcal{E}/\rho_B - M_N = -15.7$ MeV, and pressure, $P = 0$ at saturation density $\rho_B = \rho_0 = 0.15\,\text{fm}^{-3}$. Also shown are the values of the nuclear matter incompressibility K and the slope of the symmetry energy L for quark masses $m_q = 150$ MeV and $m_q = 200$ MeV.

m_q (MeV)	g_σ^q	g_ω	g_ρ	M_N^*/M_N	K (MeV)	L (MeV)
150	4.57842	6.49093	8.82263	0.85	235.55	86.20
200	4.36839	7.40592	8.73323	0.83	242.41	86.98

TABLE IV. $x_{\omega B}$ determined by fixing the potentials for the hyperons.

m_q (MeV)	$x_{\omega\Lambda}$ $U_\Lambda = -28$ MeV	$x_{\omega\Sigma}$ $U_\Sigma = 30$ MeV	$x_{\omega\Xi}$ $U_\Xi = -10$ MeV	$x_{\omega\Xi}$ $U_\Xi = -18$ MeV
150	0.87659	1.69560	0.58729	0.48628
200	0.82541	1.45353	0.52541	0.44782

ε_0. It may be noted here that we add the standard Baym-Pethick-Sutherland (BPS) EOS [52] to the EOS of the MQMC model to describe the crust of the star, where the density is significantly smaller than nuclear matter saturation density. Recent works detail the importance and technique of such core-crust matching for nonunified equations of state [53] and the dependence of the crust-core transition density on the symmetry energy [54]. Of particular importance is the maximum mass obtained from the solution of the TOV equations. The value of r $(= R)$, where the pressure vanishes defines the surface of the star. The surface gravitational redshift Z_s is defined as

$$Z_s = \left(1 - \frac{2GM}{R}\right)^{-1/2} - 1. \tag{38}$$

IV. RESULTS AND DISCUSSION

The MQMC model has two potential parameters, a and V_0, which are obtained by fitting the nucleon mass $M_N = 939$ MeV and charge radius [55] of the proton $\langle r_N \rangle = 0.84$ fm in free space. Keeping the value of the potential parameter a the same as that for nucleons, we obtain V_0 for the Λ, Δ, Σ, and Ξ baryons by fitting their respective masses to $M_\Lambda = 1115.6$ MeV, $M_\Delta = 1232$ MeV, $M_\Sigma = 1193.1$ MeV, and $M_\Xi = 1321.3$ MeV. The set of potential parameters for the baryons at zero density for quark masses $m_q = 150$ MeV and $m_q = 200$ MeV are given in Table II.

The quark meson couplings g_σ^q, $g_\omega = 3g_\omega^q$, and $g_\rho = g_\rho^q$ are fitted self-consistently for the nucleons to obtain the correct saturation properties of nuclear matter binding energy $E_{B.E.} \equiv B_0 = \mathcal{E}/\rho_B - M_N = -15.7$ MeV, pressure $P = 0$, and symmetry energy $J = 32.0$ MeV at $\rho_B = \rho_0 = 0.15$ fm^{-3}.

We have taken the standard values for the meson masses; namely, $m_\sigma = 550$ MeV, $m_\omega = 783$ MeV, and $m_\rho = 763$ MeV. The values of the quark meson couplings, g_σ^q, g_ω, and g_ρ at quark masses 150 and 200 MeV are given in Table III. The nuclear matter incompressibility values K at saturation density in the present set of parameters at quark masses $m_q = 150$ MeV and $m_q = 200$ MeV are $K = 235.55$ MeV and $K = 242.41$ MeV respectively. Recent measurements [56] extracted from doubly magic nuclei like ^{208}Pb constrain the value of K to be around 240 ± 20. Further, the slopes of the symmetry energy, $L = 86.20$ MeV and $L = 86.98$ MeV for quark masses $m_q = 150$ MeV and $m_q = 200$ MeV respectively in the present model, lie near the upper limit of the presently accepted [57] range of 58.7 ± 28.1 MeV obtained from an extensive survey of 53 analyses.

The couplings of the hyperons to the σ meson need not be fixed since we determine the effective mass of the hyperons self-consistently. The hyperon couplings to the ω meson are fixed by determining $x_{\omega B}$. The value of $x_{\omega B}$ is obtained [58–60] from the hyperon potentials in nuclear matter, $U_B = -(M_B - M_B^*) + x_{\omega B} g_\omega \omega_0$ for $B = \Lambda$, Σ, and Ξ with $U_\Lambda = -28$ MeV, $U_\Sigma = 30$ MeV and two values of U_Ξ, i.e., at $U_\Xi = -10$ MeV and $U_\Xi = -18$ MeV. For the quark masses 150 and 200 MeV with fixed $x_{\rho B} = 1$, the corresponding values for $x_{\omega B}$ for the hyperons are given in Table IV.

The Λ hyperon potential has been chosen from the measured single-particle levels of Λ hypernuclei from mass numbers $A = 3$ to 209 [40,41] of the binding of Λ to symmetric nuclear matter. Studies of Σ nuclear interaction [61,62] from the analysis of Σ^- atomic data indicate a repulsive isoscalar potential in the interior of nuclei. The Σ potential has been

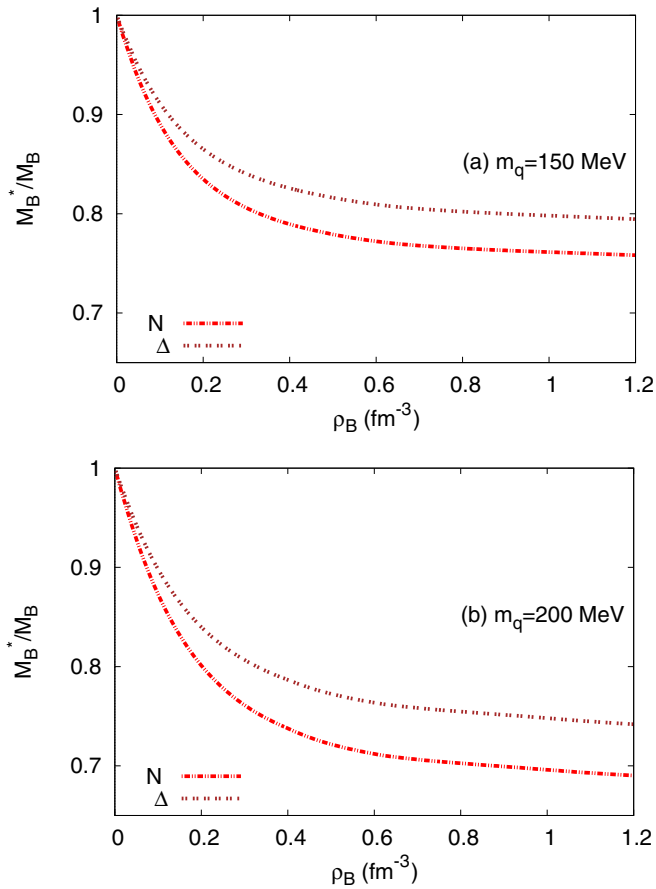

FIG. 1. Effective baryon mass as a function of baryon density at quark masses (a) $m_q = 150$ MeV and (b) $m_q = 200$ MeV.

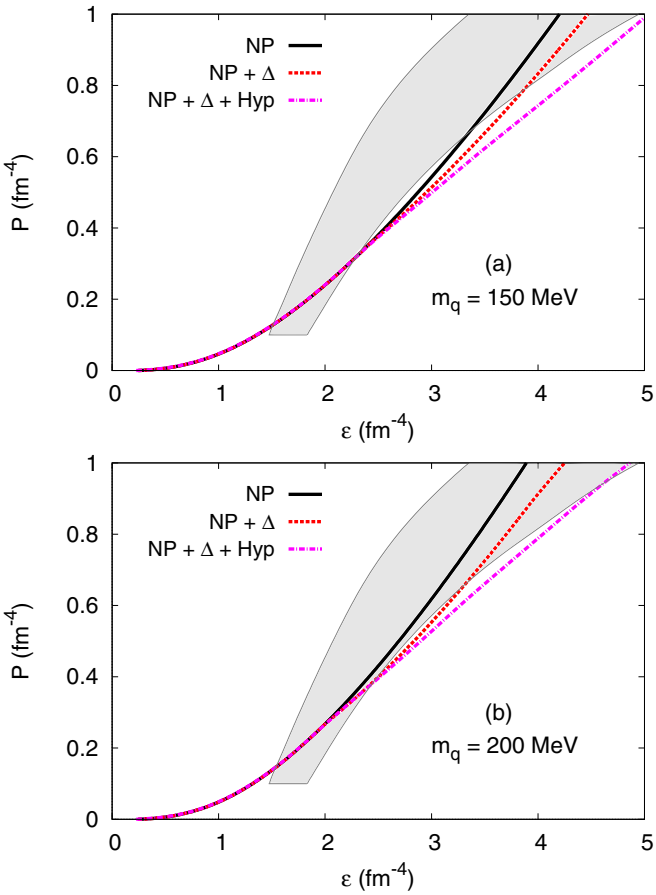

FIG. 2. Total pressure as a function of the energy density for various composition of the stellar matter at quark masses (a) $m_q = 150\,\text{MeV}$ and (b) $m_q = 200\,\text{MeV}$ with $x_{\omega\Delta} = 0.7$ and $x_{\rho\Delta} = 1$. The shaded region shows the empirical EOS obtained by Steiner *et al.* from a heterogeneous data set of six neutron stars.

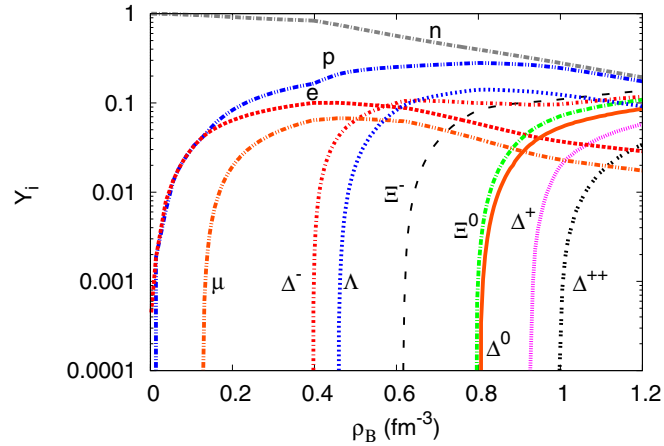

FIG. 3. Particle fraction as a function of the baryon density indicating the onset of the Δ isobars at quark mass $m_q = 200\,\text{MeV}$ and $x_{\omega\Delta} = 0.7$.

fixed at 30 MeV, as suggested from recent developments [9,11,42–44] in hypernuclear physics. Measurements of the final state interaction of Ξ hyperons produced in (K^-, K^+) reaction on ^{12}C in the E224 experiment at KEK [63] and the E885 experiment at AGS [64] indicate shallow attractive potentials $U_\Xi \sim -16\,\text{MeV}$ and $U_\Xi \sim -14$ or less, respectively. In view of this we consider the Ξ hyperon potential at $U_\Xi = -10\,\text{MeV}$. We also study the effect of the commonly used [9–11,42,43] value of the Ξ hyperon potential $U_\Xi = -18\,\text{MeV}$ on the mass and radius of neutron stars.

The couplings of the Δ resonances are constrained poorly due to their unstable nature. Earlier works [45] based on the quark counting argument considered a simple universal choice of couplings of the Δ with the mesons. Wehrberger *et al.* [47] carried out studies of Δ-baryon excitation in finite nuclei in the linear Walecka model and reproduced properties of some finite nuclei. They constrained the scaling to $0 \lesssim x_{\sigma\Delta} - x_{\omega\Delta} \lesssim 0.2$. Furthermore, suggestions [20,25] on the range of uncertainty for the Δ potential, $-30\,\text{MeV} + U_N \lesssim U_\Delta \lesssim U_N$, from the studies of electron-nucleus [47,65,66] and pion-nucleus [67,68] scattering and photoabsorption, lead to a constraint $-90 < U_\Delta < -50\,\text{MeV}$ for $U_N \simeq -(50\text{–}60)\,\text{MeV}$.

As stated in Sec. III, for the present work there is no direct definition for $x_{\sigma\Delta}$. We are therefore limited to the choice of fixing $x_{\omega\Delta}$ for obtaining Δ potential values. Moreover, our choice of the $x_{\omega\Delta}$ is also restricted by the neutron star mass constraint. In this context we choose to fix $x_{\omega\Delta} = 0.7$, since in the present model this gives the value of $U_\Delta = -96\,\text{MeV}$ for quark mass 200 MeV and $U_\Delta = -88\,\text{MeV}$ for quark mass 150 MeV, which lie close to the range obtained from photoabsorption studies. The Δ coupling to the ρ meson is fixed at $x_{\rho\Delta} = 1$. However, variations in coupling strength $x_{\omega\Delta}$ and $x_{\rho\Delta}$ have been made to study their impact on the critical density of forming Δ resonances and on the structure of neutron stars.

Figures 1(a) and 1(b) show the effective mass of the nucleons and Δ for the quarks masses $m_q = 150\,\text{MeV}$ and $m_q = 200\,\text{MeV}$ respectively. With increasing density the effective mass decreases due to the attractive σ field for the baryons. The EOS for different compositions of neutron star matter at quark masses 150 and 200 MeV are shown in Fig. 2. It is observed that, with the inclusion of Δ, the EOS becomes softer than for matter containing only nucleons. For matter containing nucleons, delta baryons, and hyperons, we observe a significant decrease of stiffness.

In fact, for matter composed of nucleons + Δ + hyperon, the stiffness of the EOS decreases with the early appearance of the Δ^- at a density of around $\rho_B = 0.39\,\text{fm}^{-3}$ for $m_q = 200\,\text{MeV}$. The hyperons start appearing at a density of $\rho_B = 0.45\,\text{fm}^{-3}$, further reducing the stiffness of the EOS. A similiar trend is also observed for quark mass $m_q = 150\,\text{MeV}$. The shaded region shows the empirical EOS obtained by Steiner *et al.* from a heterogeneous data set of six neutron stars with well determined distances [69].

The composition of the matter in terms of the particle fractions for β-equilibrated matter is shown in Fig. 3. At densities below the saturation value the β decay of neutrons to muons is allowed, and thus muons start to populate. At higher densities the lepton fraction begins to fall since charge neutrality can now be maintained more economically with the appearance of negative baryon species. Since the Δ^- can

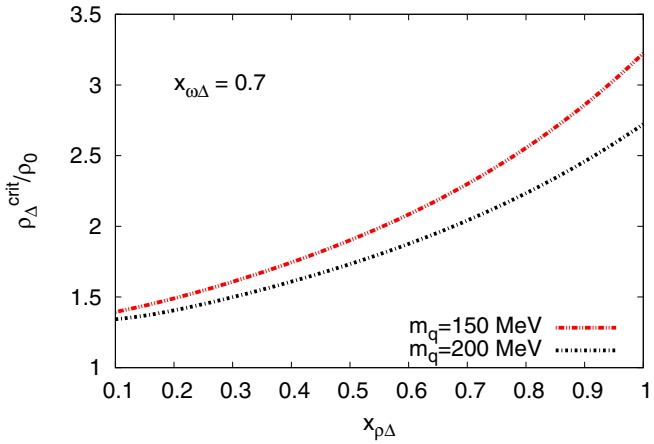

FIG. 4. Effect of variation in Δ-ρ coupling strength $x_{\rho\Delta}$ on the critical density of forming Δ^- at $x_{\omega\Delta} = 0.7$ for quark masses 150 and 200 MeV.

replace the neutron and electron at the top of the Fermi sea, it appears first at a density of $\rho_B = 0.39\,\mathrm{fm}^{-3}$. This is followed by the appearance of Λ. The sequence of appearance of the Δ resonances is consistent with the notion of charge-favored or unfavored species [1]. As such, the first Δ resonance to appear is Δ^-, followed by the Δ^0, Δ^+, and Δ^{++}. The slope of the symmetry energy L also plays a key role in the appearance of Δ resonances. By constraining L in the range $40 < L < 62$ MeV, Drago *et al.* [23] have observed the appearance of Δ at close to twice the saturation density. At high densities all baryons tend to saturate. It may be noted here that the Σ hyperon is not present in the matter distribution for the given set of potentials since we have chosen a repulsive potential for it.

Since the vector coupling of the Δ are not constrained by the properties of saturated nuclear matter, we study the effect of moderate variations in the strength of the vector coupling of the Δ on the critical density of forming Δ^- baryons and on the mass-radius relation of the neutron star. Figure 4 shows the variation in the $\rho_{\Delta^-}^{\mathrm{crit}}$ with increasing ρ-Δ coupling strength $x_{\rho\Delta}$ and a fixed value $x_{\omega\Delta} = 0.7$ for quark masses $m_q = 150$ and 200 MeV. It is observed that the value of $\rho_{\Delta^-}^{\mathrm{crit}}$ increases with an increase in the value of $x_{\rho\Delta}$.

Considering only the nucleon and Δ composition of the matter, we plot in Fig. 5 the gravitational mass as a function of radius by changing the coupling strengths $x_{\omega\Delta}$ and $x_{\rho\Delta}$ of the Δ isobars. By decreasing the coupling strength from $x_{\omega\Delta} = 1$ to $x_{\omega\Delta} = 0.6$, we observe in Fig. 5(a) a gradual decrease in the maximum mass of the star. A similar behavior is also observed in Fig. 5(b) by decreasing the $x_{\rho\Delta}$ coupling strength. The results are tabulated in Table V. This follows from the fact that, by decreasing the interaction strength of the Δ with respect to the nucleons, the EOS becomes softer with a consequent decrease in the maximum mass of the star [70]. We further observe that an increase in the Δ-ω coupling strength tends to reduce the radius while an increase in the Δ-ρ coupling strength increases the radius corresponding to the maximum mass of the neutron star. This appreciable change in the radius at maximum mass indicates a strong dependence on

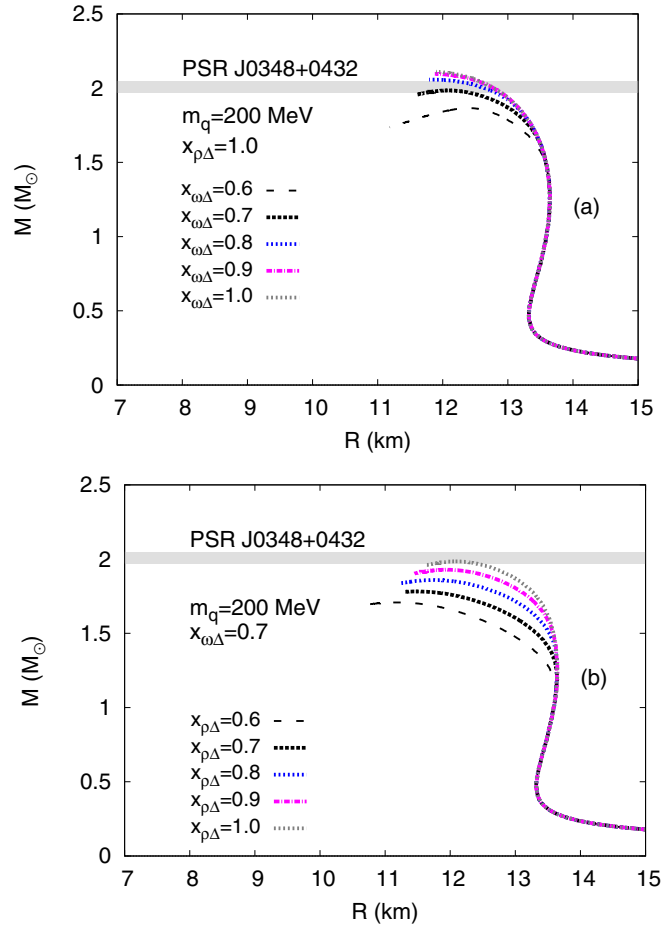

FIG. 5. Gravitational mass as a function of radius for various coupling strengths. In (a) the value of $x_{\omega\Delta}$ is varied keeping $x_{\rho\Delta} = 1$ while in (b) $x_{\rho\Delta}$ is varied keeping $x_{\omega\Delta} = 0.7$. Both are determined for $N + \Delta$ composition at a quark mass of $m_q = 200$ MeV.

the meson-baryon coupling constants. However, the radius of canonical neutron stars of $1.4M_\odot$ has almost no change.

To examine further the dependence of the Δ formation on the meson-baryon couplings, we chose a stronger ω-Δ coupling at $x_{\omega\Delta} = 1.1$, as suggested in [26], and varied the $x_{\rho\Delta}$ strength at $x_{\rho\Delta} < 1.0$. We observe that such a combination significantly changes the composition of the matter with

TABLE V. Mass-radius relation of neutron stars for different coupling strength with $N + \Delta$ matter. (a) shows the effect variation of $x_{\omega\Delta}$ at $m_q = 200$ MeV with $x_{\rho\Delta} = 1$. (b) shows the effect of variation of $x_{\rho\Delta}$ of at $m_q = 200$ MeV at a fixed value of $x_{\omega\Delta} = 0.7$

(a)				(b)			
$x_{\omega\Delta}$	$M_{\max}$ ($M_\odot$)	R (km)	$R_{1.4}$ (km)	$x_{\rho\Delta}$	$M_{\max}$ ($M_\odot$)	R (km)	$R_{1.4}$ (km)
0.60	1.86	12.40	13.6	0.60	1.70	11.18	13.2
0.70	1.98	12.08	13.6	0.70	1.78	11.47	13.5
0.80	2.05	11.82	13.6	0.80	1.85	11.74	13.6
0.90	2.09	11.87	13.6	0.90	1.92	11.93	13.6
1.00	2.11	11.89	13.6	1.00	1.98	12.08	13.6

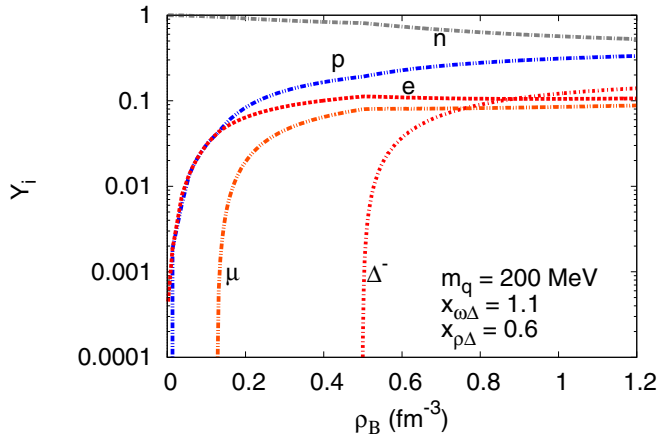

FIG. 6. Particle fraction as a function of the baryon density for the coupling values $x_{\omega\Delta} = 1.1$ and $x_{\rho\Delta} = 0.6$ at quark mass $m_q = 200$ MeV with $N + \Delta$ matter.

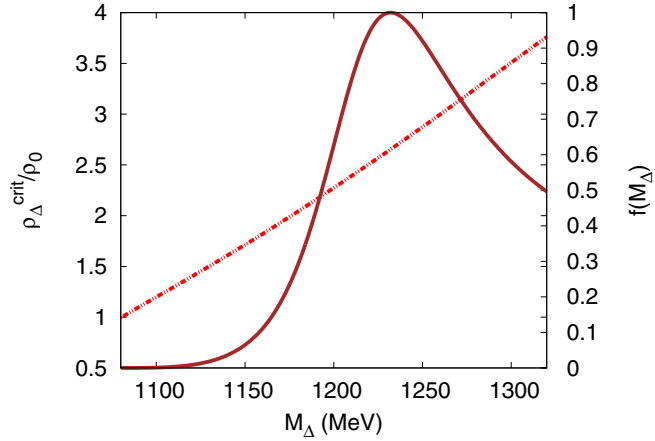

FIG. 7. Variation of critical density $\rho_{\Delta^-}^{\rm crit}$ with change in mass of Δ baryon. Also shown is the Breit-Wigner mass distribution in free space.

the appearance of only a Δ^- resonance and no other delta resonant state, even within 7–8 times the saturation density, as shown in Fig. 6. We find that with increasing strength of $x_{\rho\Delta}$, $\rho_{\Delta^-}^{\rm crit}$ shifts to higher densities. Such a trend increases the maximum mass of the neutron star, as given in Table VI. For $x_{\rho\Delta} \geqslant 1$ with $x_{\omega\Delta} = 1.1$ there is no delta formation in the neutron star matter. This indicates that in the present model stronger vector coupling strengths do not allow the the possibility of Δ formation in neutron star matter.

Since the Δ mass distribution can be modified in the nuclear medium [71,72], we plot in Fig. 7 the effect of change in $\rho_{\Delta^-}^{\rm crit}$ with variation of the Δ mass M_Δ. The Breit-Wigner mass distribution $f(M_\Delta)$ shown by Δ resonances in free space is also plotted. In free space, the Breit-Wigner mass distribution for Δ resonances is

$$f(M_\Delta) = \frac{1}{4}\frac{\Gamma^2(M_\Delta)}{\left(M_\Delta - M_\Delta^0\right)^2 + \Gamma^2(M_\Delta)/4}, \tag{39}$$

where $\Gamma(M_\Delta)$ is the mass-dependent width [73,74] given by

$$\Gamma(M_\Delta) = 0.47q^3/\left(M_\pi^2 + 0.6q^2\right)\ \text{GeV}. \tag{40}$$

Here $q = \{([M_\Delta^2 - M_N^2 + M_\pi^2]/2M_\Delta)^2 - M_\pi^2\}^{1/2}$ is the pion momentum in the Δ rest frame in the $\Delta \to \pi + N$ decay process. It is observed that low mass Δ resonances appear near $2\rho_0$, thus indicating that hyperons can appear after Δ's in neutron stars. We also show in Fig. 8 the mass-radius relation of neutron stars, for quark masses 150 and 200 MeV, with change in the mass of Δ resonances for fixed $x_{\omega\Delta} = 0.7$ and $x_{\rho\Delta} = 1$. In both Figs. 8(a) and 8(b) we observe a smaller maximum mass for low mass Δ resonances, indicating relatively more abundance due to their lower production thresholds [22].

TABLE VI. Mass-radius relation of neutron stars for fixed $x_{\omega\Delta} = 1.1$ and varying coupling strength of $x_{\rho\Delta}$ with $N + \Delta$ matter at $m_q = 200$ MeV.

$x_{\rho\Delta}$	$M_{\rm max}$ ($M_\odot$)	R (km)	$R_{1.4}$ (km)
0.60	2.08	11.85	13.6
0.70	2.10	11.89	13.6
0.80	2.11	11.90	13.6

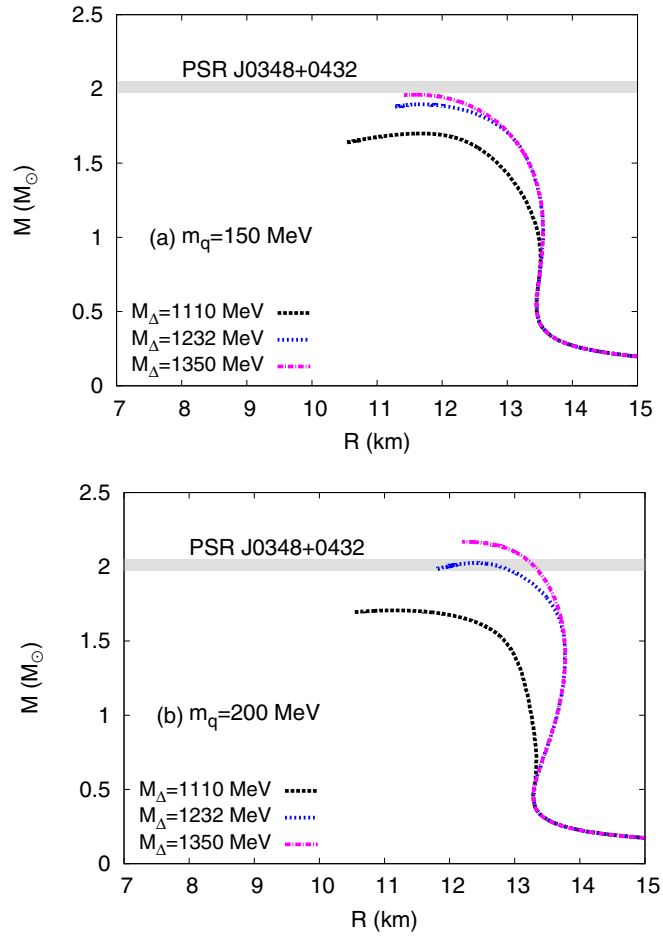

FIG. 8. Gravitational mass as a function of radius for different masses of of the Δ resonance at quark mass (a) $m_q = 150$ MeV and (b) $m_q = 200$ MeV with $x_{\omega\Delta} = 0.7$.

TABLE VII. Stellar properties obtained at different compositions of star matter for quark masses $m_q = 150$ MeV and $m_q = 200$ MeV.

Composition	$m_q = 150$ MeV				$m_q = 200$ MeV			
	$M_{\max}$ ($M_\odot$)	R (km)	ε_0 (fm^{-4})	$R_{1.4}$ (km)	$M_{\max}$ ($M_\odot$)	R (km)	ε_0 (fm^{-4})	$R_{1.4}$ (km)
N	1.97	11.41	6.34	13.4	2.11	11.89	5.45	13.6
$N + \Delta$	1.89	11.67	6.06	13.4	1.98	12.08	5.56	13.6
$N + \Delta +$ hyperons	1.82	12.15	5.28	13.4	1.90	12.41	5.02	13.6

In Fig. 9 we plot the mass-radius relations for the three compositions of neutron star matter at $m_q = 150$ MeV and $m_q = 200$ MeV with $x_{\omega\Delta} = 0.7$ and $x_{\rho\Delta} = 1$. A stiffer EOS corresponding to matter with nucleons only gives the maximum star mass of $M_{\rm star} = 2.11 M_\odot$ at $m_q = 200$ MeV. With the appearance of the Δ isobars, mass decreases by $0.13 M_\odot$ to $M_{\rm star} = 1.98 M_\odot$. The inclusion of the hyperons further softens the EOS, resulting in a corresponding decrease in the maximum mass to $M_{\rm star} = 1.90 M_\odot$. For the lower quark mass of $m_q = 150$ MeV, we observe a similar trend with a decrease in the maximum mass. The detailed results including the maximum mass, radius, central density (ε_0), and the radius corresponding to the canonical star mass $1.4 M_\odot$ ($R_{1.4}$), for the two quark masses $m_q = 150$ MeV and $m_q = 200$ MeV, are shown in Table VII. We note here that by changing the value of the U_Ξ to -18 MeV from -10 MeV we obtain a smaller maximum mass with a corresponding increase in radii. For $m_q = 200$ MeV the star mass decreases from $1.90 M_\odot$ to $1.86 M_\odot$, and the corresponding radius increases from 12.41 to 12.61 km. For $m_q = 150$ MeV the star mass decreases from $1.82 M_\odot$ to $1.77 M_\odot$ and the corresponding radius increases from 12.15 to 12.36 km.

From our calculations we obtain a range of masses varying from $2.11 M_\odot$ to $1.77 M_\odot$ depending on the composition of the matter. We note here that, for an appropriate description of the low-density crust region of the neutron star, we add to the core EOS the Baym-Pethick-Sutherland (BPS) crust EOS [52].

The radii corresponding to the maximum mass for various compositions, for the quark masses $m_q = 150$ MeV and $m_q = 200$ MeV, are shown in Table VII. We observe moderate increase in the radii from $R = 11.89$ km for matter with nucleons only to $R = 12.41$ km for matter composed of nucleons, Δ, and hyperons. Further, we obtain a radius of $R_{1.4} = 13.6$ km for a canonical neutron star of mass $1.40 M_\odot$. For the quark mass $m_q = 150$ MeV the radius decreases as compared to the radius for quark mass $m_q = 200$ MeV. The recent detection of the gravitational-wave signal from merging neutron-star binaries, GW170817 [75], has provided new insight on the range of radii of neutron stars. Various studies [76,77] have put forth a stringent limit on the radius

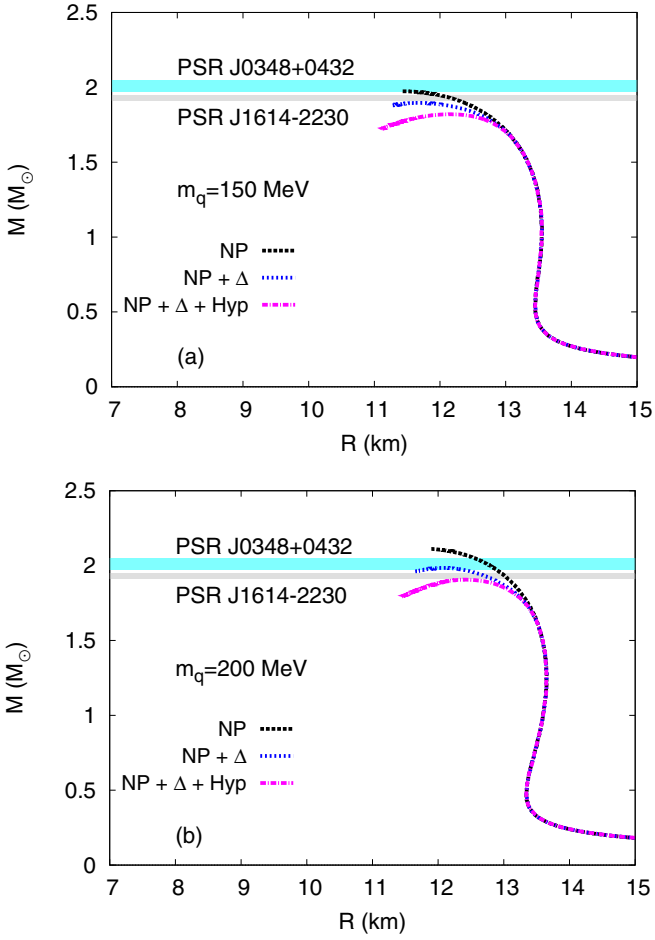

FIG. 9. Gravitational mass as a function of radius for varying composition of star matter at (a) quark mass $m_q = 150$ MeV and (b) quark mass $m_q = 200$ MeV at fixed $x_{\omega\Delta} = 0.7$.

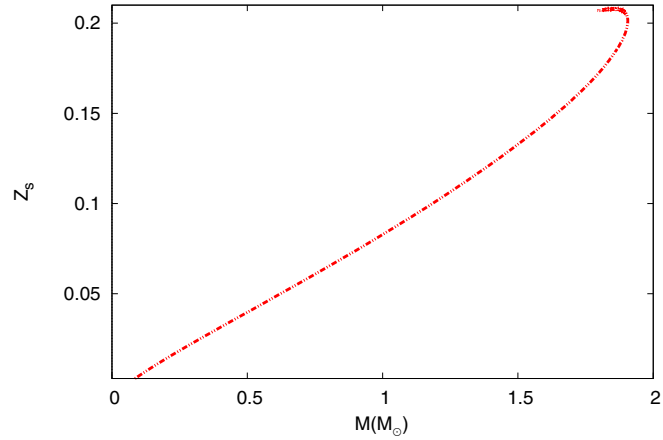

FIG. 10. Surface gravitational redshift as a function of star mass at quark mass $m_q = 200$ MeV and $x_{\omega\Delta} = 0.7$.

corresponding to the $1.4M_{\odot}$ mass neutron star, $9.9 < R_{1.4} < 13.6$ km. In the present work we obtain $R_{1.4} = 13.6$ km.

Figure 10 shows the gravitational redshift versus the gravitational mass of the neutron star at quark mass $m_q = 200$ MeV and $x_{\omega\Delta} = 0.7$. It also shows the maximum redshift (redshift corresponding to the maximum mass) which, for the present work comes out to be $Z_s^{\max} = 0.20$. This is well below the upper bound on the surface redshift for subluminal equations of state, i.e., $z_s^{CL} = 0.8509$ [78].

V. SUMMARY

In the present work we have studied the possibility of forming Δ isobars and their impact in dense matter relevant to neutron stars. We have developed the EOS using a relativistic quark model, also called the modified quark-meson coupling model, which considers the baryons to be composed of three independent relativistic quarks confined by an equal admixture of a scalar-vector harmonic potential in a background of scalar and vector mean fields. Corrections to the center-of-mass motion and pionic and gluonic exchanges within the nucleon are calculated to obtain the effective mass of the baryon. The baryon-baryon interactions are realized by the quark coupling to the σ, ω, and ρ mesons through a mean-field approximation.

By varying the composition of the matter we observe the variation in the degree of stiffness of the EOS and the corresponding effect on the maximum mass of the star. As predicted theoretically, we observe that the inclusion of the Δ and hyperon degrees of freedom softens the EOS and hence lowers the maximum mass of the neutron star. The so called Δ and hyperon puzzles state that the presence of the Δ isobars and hyperons would decrease the maximum star mass below the recently observed masses of the pulsars PSR J0348+0432 and PSR J1614−2230. In the present work, we are able to achieve the observed mass and radius constraint and at the same time satisfy the theoretical predictions of the possibility of existence of higher mass baryons in highly dense matter. Their existence, however, significantly depends on the yet unconstrained Δ-ω and Δ-ρ couplings. Such dependence on the vector couplings is studied through the effect of their variations on the critical density of forming the resonances and on the maximum mass of the star. Further, we also observe that the formation of the Δ is sensitive to the in-medium Δ mass.

ACKNOWLEDGMENTS

The authors want to acknowledge Professor Niranjan Barik for useful discussions on the preparation of the manuscript. The authors would like to acknowledge financial assistance from BRNS, India via Project No. 2013/37P/66/BRNS. P.K.P. would like to acknowledge DST, Government of India for support via Project No. SR/PST/PS-II/2017/22. B.A.L. is supported in part by the U.S. Department of Energy, Office of Science, under Grant No. DE-SC0013702, and by the National Natural Science Foundation of China under Grant No. 11320101004. H.S.S. would like to acknowledge support via CSIR-SRF Fellowship No. 09/1036/0007 (2018).

[1] N. K. Glendenning, Astrophys. J. **293**, 470 (1985).
[2] N. K. Glendenning and S. A. Moszkowski, Phys. Rev. Lett. **67**, 2414 (1991).
[3] N. K. Glendenning, *Compact Stars* (Springer-Verlag, New York, 2000).
[4] J. M. Lattimer and M. Prakash, Nucl. Phys. A **777**, 479 (2006).
[5] I. Bednarek, P. Haensel, J. L. Zdunik, M. Bejger, and R. Mańka, Astron. Astrophys. **543**, A157 (2012).
[6] T. Katayama, T. Miyatsu, and K. Saito, Astrophys. J. Suppl. Ser. **203**, 22 (2012).
[7] G. Colucci and A. Sedrakian, Phys. Rev. C **87**, 055806 (2013).
[8] T. Katayama and K. Saito, Phys. Lett. B **747**, 43 (2015).
[9] R. O. Gomes, V. Dexheimer, S. Schramm, and C. A. Z. Vasconcellos, Astrophys. J. **808**, 8 (2015).
[10] M. Oertel, C. Providência, F. Gulminelli, and A. R. Raduta, J. Phys. G **42**, 075202 (2015).
[11] L. Tolos, M. Centelles, and A. Ramos, Astrophys. J. **834**, 3 (2017).
[12] D. Chatterjee and I. Vidaña, Eur. Phys. J. A **52**, 29 (2016).
[13] M. Fortin, S. S. Avancini, C. Providência, and I. Vidana, Phys. Rev. C **95**, 065803 (2017).
[14] M. Marques, M. Oertel, M. Hempel, and J. Novak, Phys. Rev. C **96**, 045806 (2017).
[15] W. Spinella, Ph.D. thesis, Claremont Graduate University/San Diego State University, 2017.
[16] A. R. Raduta, A. Sedrakian, and F. Weber, Mon. Not. R. Astron. Soc. **475**, 4347 (2018).
[17] G. Baym, T. Hatsuda, T. Kojo, P. D. Powell, Y. Song, and T. Takatsuka, Rep. Prog. Phys. **81**, 056902 (2018).
[18] I. Vidaña, Proc. R. Soc. A **474**, 20180145 (2018).
[19] J. C. T. De Oliveira, M. Kyotoku, M. Chiapparini, H. Rodrigues, and S. B. Duarte, Mod. Phys. Lett. A **15**, 1529 (2000).
[20] A. Drago, A. Lavagno, G. Pagliara, and D. Pigato, Phys. Rev. C **90**, 065809 (2014).
[21] A. Drago, A. Lavagno, and G. Pagliara, Phys. Rev. D **89**, 043014 (2014).
[22] B.-J. Cai, F. J. Fattoyev, B. A. Li, and W. G. Newton, Phys. Rev. C **92**, 015802 (2015).
[23] A. Drago, A. Lavagno, G. Pagliara, and D. Pigato, Eur. Phys. J. A **52**, 40 (2016).
[24] Z.-Y. Zhu, A. Li, J.-N. Hu, and H. Sagawa, Phys. Rev. C **94**, 045803 (2016).
[25] E. E. Kolomeitsev, K. A. Maslov, and D. N. Voskresensky, Nucl. Phys. A **961**, 106 (2017).
[26] J. J. Li, A. Sedrakian, and F. Weber, Phys. Lett. B **783**, 234 (2018).
[27] J. Antoniadis *et al.*, Science **340**, 448 (2013).
[28] E. Fonseca *et al.*, Astrophys. J. **832**, 167 (2016).
[29] P. B. Demorest *et al.*, Nature (London) **467**, 1081 (2010).
[30] N. Barik and B. K. Dash, Phys. Rev. D **33**, 1925 (1986).
[31] N. Barik and B. K. Dash, Phys. Rev. D **34**, 2092 (1986).
[32] N. Barik and B. K. Dash, Phys. Rev. D **34**, 2803 (1986).
[33] N. Barik and R. N. Mishra, Phys. Rev. D **61**, 014002 (1999).

[34] N. Barik, R. N. Mishra, D. K. Mohanty, P. K. Panda, and T. Frederico, Phys. Rev. C **88**, 015206 (2013).
[35] R. N. Mishra, H. S. Sahoo, P. K. Panda, N. Barik, and T. Frederico, Phys. Rev. C **92**, 045203 (2015).
[36] R. N. Mishra, H. S. Sahoo, P. K. Panda, N. Barik, and T. Frederico, Phys. Rev. C **94**, 035805 (2016); **98**, 019903(E) (2018).
[37] X. Xing, J. Hu, and H. Shen, Phys. Rev. C **95**, 054310 (2017).
[38] Z.-Y. Zhu and A. Li, Phys. Rev C **97**, 035805 (2018).
[39] Z.-Y. Zhu, E.-P. Zhou, and A. Li, Astrophys. J. **862**, 98 (2018).
[40] D. J. Millener, C. B. Dover, and A. Gal, Phys. Rev. C **38**, 2700 (2001).
[41] Y. Yamamoto, H. Bando, and J. Zofka, Progr. Theor. Phys. **80**, 757 (1988).
[42] T. Miyatsu, M. K. Cheoun, and K. Saito, Phys. Rev. C **88**, 015802 (2013).
[43] L. L. Lopes and D. P. Menezes, Phys. Rev. C **89**, 025805 (2014).
[44] K. A. Maslov, E. E. Kolomeitsev, and D. N. Voskresensky, Nucl. Phys. A **950**, 64 (2016).
[45] S. A. Moszkowski, Phys. Rev. D **9**, 1613 (1974).
[46] A. Bohr and B. R. Mottelson, Phys. Lett. B **100**, 10 (1981).
[47] K. Wehrberger, C. Bedau, and F. Beck, Nucl. Phys. A **504**, 797 (1989).
[48] P. A. M. Guichon, Phys. Lett. B **200**, 235 (1988).
[49] P. A. M. Guichon, K. Saito, E. Rodionov, and A. W. Thomas, Nucl. Phys. A **601**, 349 (1996).
[50] J. R. Oppenheimer and G. M. Volkoff, Phys. Rev. **55**, 374 (1939).
[51] R. C. Tolman, Proc. Nat. Acad. Sci. USA **20**, 169 (1934).
[52] G. Baym, C. Pethick, and P. Sutherland, Astrophys. J **170**, 299 (1971).
[53] M. Fortin, C. Providência, Ad. R. Raduta, F. Gulminelli, J. L. Zdunik, P. Haensel, and M. Bejger, Phys. Rev. C **94**, 035804 (2016).
[54] N.-B. Zhang, B.-A. Li, and J. Xu, Astrophys. J. **859**, 90 (2018).
[55] R. Pohl *et al.*, Nature (London) **466**, 213 (2010).
[56] U. Garg and G. Colò, Prog. Nucl. Part. Phys. **101**, 55 (2018).
[57] B.-A. Li, Nucl. Phys. News **27**, 7 (2017).
[58] P. K. Panda, D. P. Menezes, and C. Providência, Phys. Rev. C **69**, 025207 (2004).
[59] P. K. Panda, C. Providência, and D. P. Menezes, Phys. Rev. C **82**, 045801 (2010).
[60] P. K. Panda, A. M. S. Santos, D. P. Menezes, and C. Providência, Phys. Rev. C **85**, 055802 (2012).
[61] J. Mares, E. Friedman, A. Gal, and B. K. Jennings, Nucl. Phys. A **594**, 311 (1995).
[62] S. Bart, R. E. Chrien, W. A. Franklin, T. Fukuda, R. S. Hayano, K. Hicks, E. V. Hungerford, R. Michael, T. Miyachi, T. Nagae, J. Nakano, W. Naing, K. Omata, R. Sawafta, Y. Shimizu, L. Tang, and S. W. Wissink, Phys. Rev. Lett. **83**, 5238 (1999).
[63] T. Fukuda, A. Higashi, Y. Matsuyama, C. Nagoshi, J. Nakano, M. Sekimoto, P. Tlusty, J. K. Ahn, H. Enyo, H. Funahashi, Y. Goto, M. Iinuma, K. Imai, Y. Itow, S. Makino, A. Masaike, Y. Matsuda, S. Mihara, N. Saito, R. Susukita, S. Yokkaichi, K. Yoshida, M. Yoshida, S. Yamashita, R. Takashima, F. Takeutchi, S. Aoki, M. Ieiri, T. Iijima, T. Yoshida, I. Nomura, T. Motoba, Y. M. Shin, S. Weibe, M. S. Chung, I. S. Park, K. S. Sim, K. S. Chung, and J. M. Lee, Phys. Rev. C **58**, 1306 (1998).
[64] P. Khaustov, D. E. Alburger, P. D. Barnes, B. Bassalleck, A. R. Berdoz, A. Biglan, T. Burger, D. S. Carman, R. E. Chrien, C. A. Davis, H. Fischer, G. B. Franklin, J. Franz, L. Gan, A. Ichikawa, T. Iijima, K. Imai, Y. Kondo, P. Koran, M. Landry, L. Lee, J. Lowe, R. Magahiz, M. May, R. McCrady, C. A. Meyer, F. Merrill, T. Motoba, S. A. Page, K. Paschke, P. H. Pile, B. Quinn, W. D. Ramsay, A. Rusek, R. Sawafta, H. Schmitt, R. A. Schumacher, R. W. Stotzer, R. Sutter, F. Takeutchi, W. T. H. vanOers, K. Yamamoto, Y. Yamamoto, M. Yosoi, and V. J. Zeps, Phys. Rev. C **61**, 054603 (2000).
[65] V. Koch, Int. J. Mod. Phys. E **06**, 203 (1997).
[66] J. S. O'Connell and R. M. Sealock, Phys. Rev. C **42**, 2290 (1990).
[67] Y. Horikawa, M. Thies, and F. Lenz, Nucl. Phys. A **345**, 386 (1980).
[68] S. X. Nakamura, T. Sato, T. S. H. Lee, B. Szczerbinska, and K. Kubodera, Phys. Rev. C **81**, 035502 (2010).
[69] A. W. Steiner, J. M. Lattimer, and E. F. Brown, Astrophys. J **722**, 33 (2010).
[70] T. Schurhoff, S. Schramm, and V. Dexheimer, Astrophys. J. Lett. **724**, L74 (2010).
[71] G. E. Brown and W. Weise, Phys. Rep. **22**, 279 (1975).
[72] H. Lenske, talk at the NUSTAR Collaboration Meeting, March 2014, Darmstadt, https://indico.gsi.de/event/2354/session/22/contribution/34/material/slides/0.pdf
[73] Y. Kitazoe, M. Sano, H. Toki, and S. Nagamiya, Phys. Lett. B **166**, 35 (1986).
[74] B. A. Li, Nucl. Phys. A **552**, 605 (1993).
[75] B. P. Abbott *et al.* (LIGO Scientific and Virgo Collaboration), Phys. Rev. Lett. **119**, 161101 (2017).
[76] E. Annala, T. Gorda, A. Kurkela, and A. Vuorinen, Phys. Rev. Lett. **120**, 172703 (2018).
[77] P. G. Krastev and B. A. Li, arXiv:1801.04620.
[78] P. Haensel, J. P. Lasota, and J. L. Zdunik, Astron. Astrophys. **344**, 151 (1999).